60, 4466 (1974).
[6]P. Pyykkö and J. P. Desclaux, Nature (London) 226, 336 (1977).
[7]D. E. Ellis and G. S. Painter, Phys. Rev. B 2, 2887 (1970).
[8]A. Rosén, D. E. Ellis, H. Adachi, and F. W. Averill, J. Chem. Phys. 65, 3629 (1976).
[9]A. Rosén and D. E. Ellis, Z. Phys. A283, 3 (1977).
[10]W. Moffit, G. L. Goodman, M. Fred, and B. Weinstock, Mol. Phys. 2, 109 (1959).
[11]J. C. Slater, *The Self-Consistent Field for Molecules and Solids* (McGraw-Hill, New York, 1972).
[12]G. S. Hurst, M. H. Nayfeh, and J. P. Young, Appl. Phys. Lett. 30, 229 (1977).
[13]W. M. Fairbank, T. W. Hänsch, and A. L. Schawlow, J. Opt. Soc. Am. 65, 199 (1975).

Vortex Waves: Stationary "V States," Interactions, Recurrence, and Breaking

Gary S. Deem
Bell Laboratories, Wippany, New Jersey 07981

and

Norman J. Zabusky
University of Pittsburgh, Pittsburgh, Pennsylvania 15260
(Received 29 December 1977)

We have found a class of stationary translating and stationary rotating solutions to the Euler equations in two dimensions—a Hamiltonian system. These "V states" are nonlinear dispersive waves that seem to play a role in our observation of long-time recurrence and breaking phenomena.

We have found a class of uniformly rotating and uniformly translating solutions to the Euler equations in *two dimensions* that we call "V states." The set of uniformly rotating V states, $V(m,T)$, are single, finite-area vortex regions (FAVR's) of constant vorticity density, having m-fold symmetry and period T. They are natural extensions of the Kirchhoff vortex,[1] an elliptical ($m=2$) FAVR of constant vorticity density. The set of uniformly translating V states, $V_{tr}(L,U)$, are two oppositely signed FAVR's of constant vorticity density having centers of area separated by L and having speed U. They are generalizations of two oppositely signed point vortices. The boundaries of the rotating V states are *nonlinear dispersive waves* and seem to play a role in our observations of long-time recurrence phenomena for perturbations to a circular FAVR.

The Euler equations in two dimensions are a Hamiltonian system and can be written in the vorticity-stream function variables as

$$\partial_t\zeta + u\partial_x\zeta + v\partial_y\zeta = 0, \quad \partial_{xx}\psi + \partial_{yy}\psi = -\zeta, \qquad u = \partial_y\psi, \quad v = -\partial_x\psi. \tag{1}$$

Lamb shows[2] that a small-amplitude perturbation to a circular region of constant vorticity density ζ_0 of the form

$$r = R_0[1 + \epsilon\cos(m\alpha - \tilde{\omega}_m t)] \tag{2}$$

has the linear dispersion relation (designated by a tilde)

$$\tilde{\omega}_m = \tfrac{1}{2}\zeta_0(m-1). \tag{3}$$

The angular velocity of the mth mode in the laboratory frame is

$$\dot{\tilde{\alpha}} = \tilde{\omega}_m/m = \tfrac{1}{2}\zeta_0(m-1)/m. \tag{4}$$

For example, $m=2$ waves rotate in the same direction and with *half* the speed[1] of fluid particles at the boundary. Higher-m modes have a smaller period of rotation

$$\tilde{T}_m = 2\pi/\dot{\tilde{\alpha}}_m = 4\pi m/\zeta_0(m-1). \tag{5}$$

These points of the linear dispersion relation are the open circles on Fig. 1.

As Lamb reports,[1] the elliptical boundary has a period $T_2(b/a) = (2\pi/\zeta_0)(b+a)^2/ba$, a function of the ratio of the major to minor axes (b/a). This *band* of periods is given in Fig. 1 as the vertical line at $m^{-1}=0.5$ that emanates upward from $(T\zeta_0/2\pi)=4.0$. For $(b/a)\to\infty$ one expects these stationary near-sheet vortex states to be (Helmholtz) unstable to small perturbations.

The contour-dynamics (CD) algorithm[3] treats interactions among regions of *constant* vorticity density and thereby obtains a unit reduction in dimension. Using the two-dimensional Green's function, $\ln r$, the Poisson equation is inverted

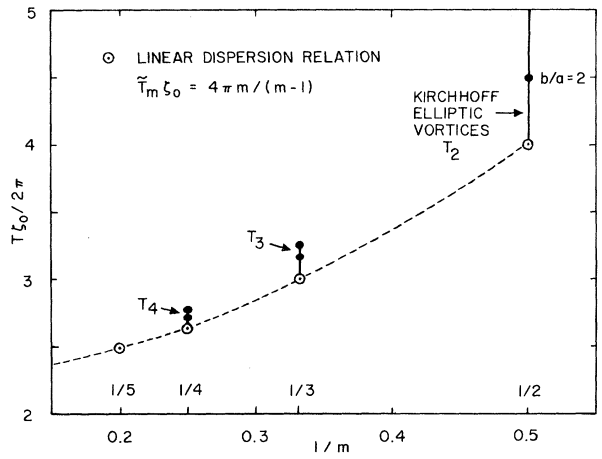

FIG. 1. Rotational periods for V states of the Euler equations $T\zeta_0/2\pi$ vs $1/m$.

and the stream function is $\psi = (-\frac{1}{2}\pi)\int\int d\xi\, d\eta \ln r \times \zeta(\xi,\eta)$, where $r = [(x-\xi)^2 + (y-\eta)^2]^{1/2}$. The velocity $\vec{u} = u\vec{e}_x + v\vec{e}_y$ of each point on a contour Γ is obtained by differentiating ψ. Since $\zeta(\xi,\eta)$ is a piecewise-constant function, the area integral is converted to a line integral over Γ, or

$$\vec{u}(x,y) = \zeta_0 \oint_\Gamma \ln r(\vec{e}_x d\xi + \vec{e}_y d\eta). \tag{6}$$

The time evolution of points (x,y) on Γ is then determined by the differential equations $(\dot{x}\vec{e}_x + \dot{y}\vec{e}_y) = \vec{u}(x,y)$.

We began this investigation by seeking bands on the $(T\zeta_0/2\pi)$ versus m^{-1} diagram that emanate upward from the open circles at integer m. To accomplish this, we substituted the discretized equations of the CD algorithm[3] into the equation for a uniformly rotating boundary, namely, $\vec{n} \cdot \vec{V}_{\text{particle}} = \vec{n} \cdot \vec{V}_{\text{boundary}}$ or

$$\partial\psi/\partial s = -\Omega r\, dr/ds, \tag{7}$$

evaluated at the boundary $r = R(x_\Gamma, y_\Gamma) = \boldsymbol{R}(\alpha)$, where r, α, s, and $\vec{n}$ are the polar coordinates, are length, and unit normal vector to the boundary. $\Omega = 2\pi/T$, the angular velocity of the boundary, is a bifurcation parameter. If we substitute $\partial_s\psi = u\sin\theta - v\cos\theta$ in Eq. (7), and rearrange we obtain

$$F \equiv [u\sin\theta - v\cos\theta + \Omega R(dR/da)]_\Gamma = 0, \tag{8}$$

where $\tan\theta = dy/dx$ is the local slope of the contours. If one assumes a single-valued contour $r = R(\alpha)$, Eq. (6) can be written as

$$\vec{u} = \zeta_0 \oint_r d\beta\, R(\beta)(\ln r)[\vec{e}_x(\cos\beta - Q\sin\beta) + \vec{e}_y(\sin\beta + Q\cos\beta)], \tag{9}$$

where $Q(\alpha) = R^{-1}dR/D\alpha$, and $r = [R^2(\alpha) + R^2(\beta) - 2R(\alpha)R(\beta)\cos(\beta-\alpha)]^{1/2}$, and Eq. (7) can be written as the nonlinear integro-differential equation for $R(\alpha)$

$$4\pi\Omega dR/d\alpha = \zeta_0 \int_0^{2\pi} d\beta\, R(\beta)(\ln r^2)\{\sin(\beta-\alpha)[1 + Q(\alpha)Q(\beta)] + \cos(\beta-\alpha)[Q(\alpha) - Q(\beta)]\}. \tag{10}$$

For V states translating uniformly with velocity U, the equation corresponding to (8) is

$$G = [(u-U)\sin\theta - v\cos\theta]_\Gamma = 0. \tag{11}$$

Note that u and v now have contributions from both contours of the translating pair of the form Eq. (6).

For a given $T(\Omega)$ or U, the solutions of Eq. (8) or Eq. (11), respectively, are the V states we are seeking. The numerical results presented in Fig. 2 have been obtained by a Newton-Raphson *iterative* computational procedure using a discretized representation of Eq. (8) or Eq. (11) with u and v given by a discretized version of Eq. (6).[3] Table I summarizes the parameters for the computation and the leading properties of the V states, including the magnitude $|\rho_m|$ and phase $\varphi_m = m(\delta\varphi)_m$ of the Fourier decomposition of $R(\alpha)$ from the center of area, where

$$\rho_m = (2\pi)^{-1}\int_0^{2\pi} e^{-im\alpha} R(\alpha) d\alpha$$
$$\varphi_m = \tan^{-1}(\mathrm{Im}\rho_m/\mathrm{Re}\rho_m). \tag{12}$$

Note, that as one proceeds away from the open circles in Fig. 1, the V-state maxima evolve toward cusps. This is seen by the increasing ratio of circumference to area or major radius to minor radius and, for example, by the negative radius of curvature in $V(4,17.5)$. The circulation (ζ_0 times area) of the translating FAVR pair $V_{tr}(2.475, \frac{1}{3})$ in Fig. 2(e) is 5.974. For two point vortices with this circulation, separated by 2.475, the translational velocity is 0.384 $[= 5.974/(2\pi \times 2.475)]$.

We have validated the fact that $V(4,17.5)$ is a stationary state by using it as the initial condition

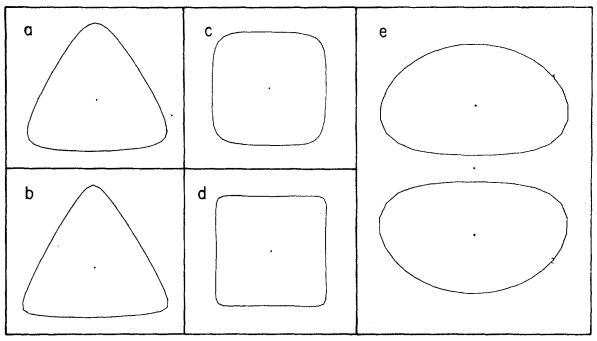

FIG. 2. Higher symmetry states. Rotating: (a) $V(3, 20.0)$, (b) $V(3,20.5)$, (c) $V(4,17.0)$, (d) $V(4,17.5)$. Translating: (e) $V_{tr}(2.475, 1/3)$.

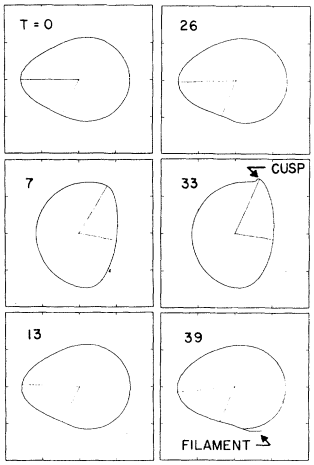

FIG. 3. Recurrence and breaking of a perturbed circular vortex $R(\alpha, 0) = R_0\{1 + \epsilon \operatorname{sech}^2[(\pi-\alpha)/\Delta\alpha]\}$ where $\Delta\alpha = \pi/6$, $\epsilon = 0.6$. The profile of $R(\alpha, t)$ is shown at times $t = 0$, 7, 13, 26, 33, and 39.

for the CD code. During one revolution the circumference exhibits a near-periodic motion, initially decreasing from 8.685 to a minimum of 8.631 (at $t = 1.475$), then increasing to a maximum of 8.747 at $t = 12.675$ and decreasing to its initial value at $t = 17.375$. The lack of exact stationarity results primarily because the initial state is not the exact stationary state, as we accept convergence from the iteration procedure when F in Eq. (8) is < 0.001. Similarly we have also validated that the translating FAVR pair in Fig. 2(e) is a stable stationary state by computing with the CD algorithm for $0 \leq t \leq 30$.

It is reasonable to conjecture that there exists a *continuum* of m-fold symmetric V states corresponding to points in bands emanating upward from the linear dispersion relation (e.g., open circles at integer m) on Fig. 1. Computational and analytical work is in progress to characterize the bands.

The above-observed near-recurrence in circumference prompted us to study strong-interaction behavior of surface modes. We perturbed a circular FAVR and used

$$R(\alpha) = R_0\{1 + \epsilon \operatorname{sech}^2[(\pi - \alpha)/\Delta\alpha]\},$$

as an initial state, where $\Delta\alpha = \pi/6$ and $\epsilon = 0.6$. The results obtained with the CD algorithm at six different times are shown in Fig. 3 with the major and minor radii indicated. The first near recurrence is at about $t = 13$ and the second at $t = 26$. Note that at $t = 33$ we see the first signs of "breaking" and filament development. If ϵ is in-

TABLE I. Features of rotating V states, $V(m,T)$, and translating V states, $V_{tr}(L,U)$, shown in Fig. 2 ($\xi_0 = 1.0$).

								MODES OF THE BOUNDARY [c]				
TYPE	NODES N	AREA [a]	CIRCUMFERENCE [a]	MAJOR RAD. [b]	MINOR RAD. [b]	$(\delta\phi)_m$ deg.	ρ_0	$\lvert\rho_m\rvert$	$\lvert\rho_{2m}\rvert$	$\lvert\rho_{3m}\rvert$	$\lvert\rho_{4m}\rvert$	$\lvert\rho_{5m}\rvert$
V(3,20.0)	60	5.000	8.615	1.591	1.056	7.19°	1.250	$1.197\ 10^{-1}$	$3.04\ 10^{-2}$	$1.02\ 10^{-2}$	$3.9\ 10^{-3}$	$1.6\ 10^{-3}$
V(3,20.5)	60	5.000	8.948	1.684	1.032	7.19°	1.245	$1.366\ 10^{-1}$	$4.17\ 10^{-2}$	$1.71\ 10^{-2}$	$8.1\ 10^{-3}$	$4.2\ 10^{-3}$
V(4,17.0)	60	5.000	8.224	1.403	1.155	19.69°	1.259	$6.02\ 10^{-2}$	$1.00\ 10^{-2}$	$2.2\ 10^{-3}$	$5.9\ 10^{-4}$	—
V(4,17.5)	60	5.000	8.685	1.523	1.117	19.69°	1.255	$8.78\ 10^{-2}$	$2.41\ 10^{-2}$	$9.3\ 10^{-3}$	$4.3\ 10^{-3}$	—
V(2.475,1/3)	40 [d]	5.974 [d]	9.155 [d]	1.791 [d]	0.987 [d]	—	—	—	—	—	—	—

[a] Area $= \sum_1^N y_n(\Delta x)_n$; circumference $= \sum_1^N (\Delta s)_n = \sum_1^N h_n$.
[b] With respect to the center of area.
[c] $R(\alpha) = \rho_0 + 2\sum_1^\infty |\rho_{pm}| \cos m[\alpha + (\delta\varphi)_m]$ (up to a rotation).
[d] Of either upper or lower FAVR.

creased breaking occurs sooner.

Via computations, we have demonstrated the existence of V states—a new class of stationary nonlinear dispersive wave solutions of the Euler equations in two dimensions. The analytic solution to this bifurcation problem may be obtained from the nonlinear integro-differential equation (10) or by the methods of complex analysis. The stability of V states to small perturbations of arbitrary symmetry is an open question.

The authors acknowledge stimulating conversations with M. D. Kruskal. The work was supported by the Office of Naval Research Contract No. NR 062-583. One of us (N.J.Z.) acknowledges the hospitality of the Program in Applied Mathematics at Princeton University during September through December 1977.

[1]H. Lamb, *Hydrodynamics* (Dover, New York, 1932), 6th ed., Sect. 159, p. 232.

[2]H. Lamb, *Hydrodynamics* (Dover, New York, 1932), Sect. 158, p. 231.

[3]N. J. Zabusky, M. H. Hughes, and K. V. Roberts, "Contour Dynamics for the Euler Equations in Two Dimensions" (to be published). The present improved version of the code uses the following N-node discretized version of Eq. (6):

$$\vec{u}(x_m, y_m) = \sum_1^N \Delta u_n (\vec{e}_x \cos\theta_n + \vec{e}_y \sin\theta_n),$$

where Δu_n is obtained by integrating Eq. (6) over a straight line segment of slope $\tan\theta_n$ which connects nodes n and $n+1$. The $2N$ differential equations

$$(\dot{x}_m \vec{e}_x + \dot{y}_m \vec{e}_y) = \vec{u}(x_m, y_m) \quad (m = 1, 2, \ldots, N)$$

are advanced in time using a second-order predictor-corrector algorithm.

Optical Coherent Transients by Laser Frequency Switching: Subnanosecond Studies

Ralph G. DeVoe and Richard G. Brewer
IBM Research Laboratory, San Jose, California 95193
(Received 23 January 1978)

By extending the laser-frequency-switching technique to a 100-psec time scale, we have observed for the Na D_1 line the first-order free-induction decay, its inhomogeneous dephasing time T_2^*, its interference with the nonlinear free-induction decay, and a 1.8-GHz interference beat of the ground-state hfs. Detailed theoretical predictions of these new coherence effects are faithfully observed.

The method of *laser frequency switching*,[1] utilized recently in generating coherent optical transients, has provided new ways for examining the dynamic interactions occurring in molecules,[1] solids,[2] and atoms.[3] In this work, the frequency of a cw dye laser is abruptly switched by means of voltage pulses applied to an intracavity electro-optic phase modulator. A resonant sample in the path of this light exhibits coherent transients which are detected in the forward beam, allowing dephasing and population decay times to be measured thus far in the range 1 μsec to 5 nsec.

In the present study, laser frequency switching is extended to a time scale of 100 psec. This fiftyfold increase in time resolution is achieved without sacrificing the previous advantages of heterodyne detection, high sensitivity, and the ability to monitor the entire class of coherent optical transients by preselecting the voltage pulse sequence. Hence, quantitative studies of coherent optical transients in this time domain are now feasible.

New coherence effects may also arise at these short times as illustrated here for the optical free-induction decay[4] of an inhomogeneously broadened transition. This transient displays a polarization containing both a first-order and a nonlinear laser field dependence having different decay times, heterodyne beat frequencies, and laser tuning characteristics. The first-order free-induction decay (FID), which was predicted,[5] decays rapidly in the time of an inverse inhomogeneous linewidth T_2^* and is observed in the time domain for the first time by laser frequency switching. The well-known nonlinear FID[4] may be long-lived with a decay time determined by the power-broadened homogeneous linewidth. We view these two forms of FID as the transient analogs of steady-state linear and nonlinear (hole-burning) laser spectroscopy of an inhomogeneously broadened transition. Furthermore, the increased time resolution permits the first observations of very-high-frequency interference beats, for example, due to the 1.8-GHz hfs splitting of